Title

Ruddlesden-Popper Phase in Two-Dimensional Inorganic Halide Perovskites: A Plausible Model and the Supporting Observations.

Journal

Nano letters, 17(9)

ISSN

1530-6984

Authors

Yu, Yi
Zhang, Dandan
Yang, Peidong

Publication Date

2017-09-01

DOI

10.1021/acs.nanolett.7b02146

Peer reviewed

NANO LETTERS

Letter

pubs.acs.org/NanoLett

Ruddlesden–Popper Phase in Two-Dimensional Inorganic Halide Perovskites: A Plausible Model and the Supporting Observations

Yi Yu,[†,‡] Dandan Zhang,[†,‡] and Peidong Yang*[,†,‡,§,∥]

[†]Department of Chemistry, [∥]Department of Materials Science and Engineering, University of California, Berkeley, California 94720, United States

[‡]Materials Sciences Division, Lawrence Berkeley National Laboratory, Berkeley, California 94720, United States

[§]Kavli Energy NanoScience Institute, Berkeley, California 94720, United States

Supporting Information

ABSTRACT: A Ruddlesden–Popper (RP) type structure is well-known in oxide perovskites and is related to many interesting properties such as superconductivity and ferroelectricity. However, the RP phase has not yet been discovered in inorganic halide perovskites. Here, we report the direct observation of unusual structure in two-dimensional $CsPbBr_3$ nanosheets which could be interpreted as the RP phase based on model simulations. Structural details of the plausible RP domains and domain boundaries between the RP and conventional perovskite phases have been revealed on the atomic level using aberration-corrected scanning transmission electron microscopy. The finding marks a major advance toward future inorganic halide RP phase synthesis and theoretical modeling, as well as unraveling their structure–property relationship.

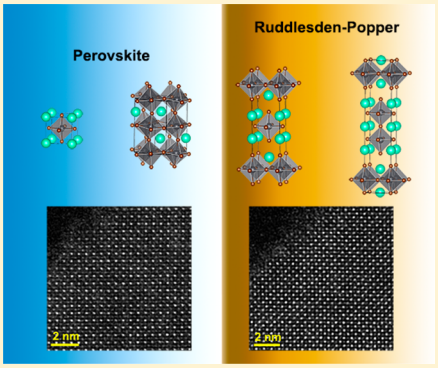

KEYWORDS: *Ruddlesden–Popper phase, inorganic halide perovskite, aberration-corrected scanning transmission electron microscopy, two-dimensional, domain*

Oxide perovskites have been intensively studied for a long time owing to their wide applications as electronic and magnetic functional materials. Apart from the original ABO_3 structure, the oxide compounds show an enormous variety of structural modifications and variants. For example, one of the important variants is the layered perovskite oxides $A_{n+1}B_nO_{3n+1}$ (n = 1, 2, ...), consisting of alternated ABO_3 and AO layers, which is also known as the Ruddlesden–Popper (RP) phase.[1] Remarkably, many interesting properties in oxide perovskites are introduced by the layered RP variants. From high T_C superconductors[2] to colossal magnetoresistance materials,[3] and to ferroelectrics,[4,5] although the understanding of the underneath structure–property relationship has not been fully reached yet, it is believed that RP structure plays a key role in it. Over the years, research on RP phase oxide perovskites is still ongoing, however, getting slower. On the other hand, halide perovskites ABX_3 (X = Cl, Br, I) have recently seen a significant revival based on the discovery of their enormous potential for photovoltaic cells. In particular, high-efficiency solar cells with improved stability based on hybrid RP phase halide perovskites have been reported very recently.[6] Therefore, it could be fascinating to pursue the research on RP phase in halide perovskites. Currently, for the synthesis of RP phase halide perovskites, there are only reports on hybrid organic–inorganic compounds.[6−8] In the past two years, hybrid halide perovskite bulk crystals[7] and thin films[6] have been successfully fabricated, and atomically thin two-dimensional (2D) hybrid nanosheets were also reported.[8] However, in the hybrid RP phase, due to the long organic chains in the organic spacing layer, the adjacent inorganic perovskite layers show hardly any electronic coupling when the organic chain is longer than propyl amine,[9] rendering similar optical properties between the bulk and the atomically thin hybrid RP phase samples.[8] Replacing the thick organic spacing layer with a thinner inorganic rock-salt layer will provide moderate interaction between the adjacent perovskite layers, thus may result in new intriguing properties that are distinct from both the three-dimensional (3D)-connected conventional perovskite and the electronically uncoupled hybrid layered RP phase. So far, all-inorganic RP phase halide perovskites have not been discovered yet. In addition, as to the atomic-scale characterization of RP phase, transmission electron microscopy (TEM) has only been demonstrated on the RP phase of oxide perovskites.[10−12] By contrast, atomic-level characterization of RP phase halide perovskites is still missing, no matter hybrid or inorganic cases.

In this work, we report the direct observation of an unusual structure in 2D all-inorganic $CsPbBr_3$ nanosheets (NSs) which cannot be interpreted as simple perovskite but could plausibly be RP phase. Atomic structures of the conventional perovskite phases as well as the plausible RP phases are clearly revealed by

Received: May 22, 2017
Revised: August 1, 2017
Published: August 10, 2017

DOI: 10.1021/acs.nanolett.7b02146
Nano Lett. 2017, 17, 5489−5494

state-of-the-art aberration-corrected scanning transmission electron microscopy (AC-STEM). The RP domains and domain boundaries are studied in detail. Combined with image simulations, further support of RP phases is achieved, while the connection and configuration of the coexisting RP and perovskite phases are discussed.

Schematics of the 3D structure models as well as the [001] projections of both conventional $CsPbBr_3$ perovskite phases and RP phases are shown in Figure 1. For $CsPbBr_3$, the crystal

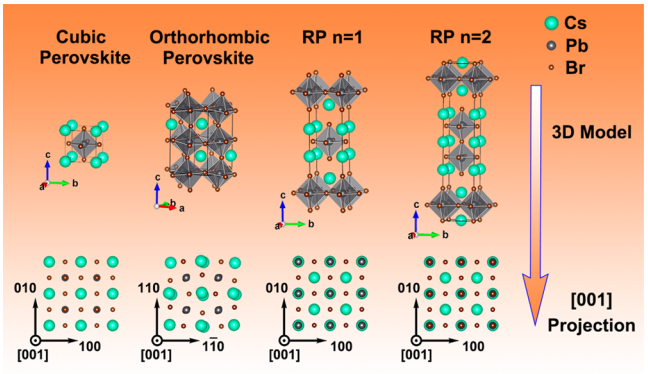

Figure 1. Schematics of the crystal structures of conventional $CsPbBr_3$ perovskite phases (cubic and orthorhombic) and RP phases (n = 1, 2). Unit cells as well as their corresponding [001] structural projections are provided. In conventional perovskite phases, the [001]-projected cation atom columns are pure Cs and Pb−Br columns, respectively. In RP phases, all the [001]-projected cation atom columns are composed of Cs−Pb−Br columns.

structure undergoes a transition from cubic to orthorhombic phase as the temperature decreases to room temperature, accompanied by the tilting of $PbBr_6$ octahedrons. For RP phases, similar to the oxide case, the general formula for halide system is $A_{n+1}B_nX_{3n+1}$. Specific to the Cs−Pb−Br system, the parent structure of the RP compounds is the cubic perovskite $CsPbBr_3$ and the cubic rock-salt type CsBr. Therefore, the formula $Cs_{n+1}Pb_nBr_{3n+1}$ can also be written as $CsBr(CsPbBr_3)_n$, which is composed of layers of n $CsPbBr_3$ unit cells that are separated by an additional CsBr layer. This structural feature is clearly seen from the n = 1 and n = 2 RP phases as demonstrated in Figure 1. The RP phases can also be considered as a regularly built-in extrinsic stacking fault, created by shifting two adjacent $CsPbBr_3$ units by an in-plane lattice vector (1/2 1/2) against each other. Since there is no any experimental report of inorganic RP phase halide perovskites so far, the RP structures shown here were obtained from first-principle calculations based on the density-functional theory (DFT).[13]

In our experiments, 2D $CsPbBr_3$ NSs were synthesized via a catalyst-free, solution-phase method, in which case most of the 2D NSs were crystallized in conventional perovskite phases.[14,15] Figure 2a shows the typical low magnification STEM morphology of the squared 2D NSs. As halide perovskites are beam-sensitive materials so that the electron beam−sample interaction should be carefully controlled, which is discussed in detail in the SI and also ref 15. According to our preliminary observations, many of the 2D thin NSs are crystallized in the cubic perovskite phase, and domains of orthorhombic phase also exist.[15] Surprisingly, in our follow-up research, we have discovered unusual domains in some of the thick NSs, which show different patterns in high-resolution STEM images compared to conventional perovskite phases. Figure 2b depicts the high-resolution AC-STEM image of the conventional $CsPbBr_3$ perovskite phase within a NS. In this Z-contrast image, heavier Pb−Br atom columns show the highest brightness, and lighter Cs atom columns are located at the center of the cube of four Pb−Br columns, showing weaker brightness. As can be seen from Figure 1, the distinguishable feature between cubic and orthorhombic perovskite phases in the [001] projection is the positions of Br atom columns. In the cubic structure the Br atom columns locate in the center of two neighboring Cs atom columns while they are off-center in the orthorhombic phase owing to the tilting of $PbBr_6$ octahedrons. A comparison between cubic and orthorhombic structures has been detailed in our early report.[15] Moreover, distinguishing the Br positions is not an easy task here as Br atom columns in the STEM images show very weak contrast and sometimes even invisible. Since we focus on the RP phases in the present work, in the following we do not make deliberate distinction of these two conventional perovskite phases and simply treat them as one perovskite phase in general. Different from the perovskite phase, Figure 2c shows the AC-STEM image of an unusual phase region, in which both the cation atom columns show high contrast. This agrees with the feature of RP phases and can be understood from the structural projections shown in Figure 1. For RP phases, as there is an in-plane (1/2 1/2) shift between two adjacent $CsPbBr_3$ units; therefore, in the [001] projection, the cation atom columns all become Cs−Pb−Br columns, despite the number n. Hence, the difference between RP and perovskite phases can be distinguished from the cation atom column intensities.

Upon knowing the structural features of both perovskite and RP phases, we further explore their distribution within the NSs. A typical morphology of the atomic structure of the NS is depicted in Figure 3a. Domain patterns can be observed, where the lower region is perovskite phase and the plausible RP phase occupies the upper region. Domain boundaries between different phases can be clearly seen. Here, we label four typical

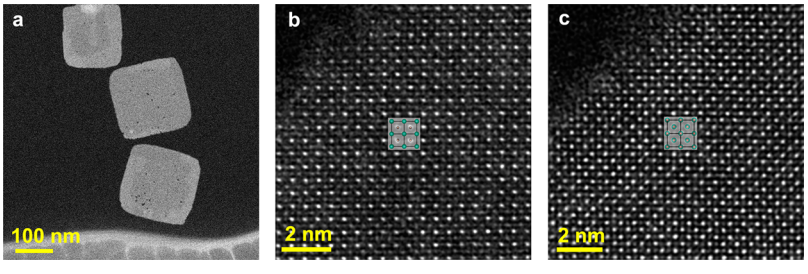

Figure 2. STEM images of the conventional perovskite phase and plausible RP phase. (a) Low magnification morphology of the 2D NSs. (b,c) Atomic-scale AC-STEM image of the conventional perovskite phase (b) and RP phase (c). [001] structure projections are overlaid in the center.

DOI: 10.1021/acs.nanolett.7b02146
Nano Lett. 2017, 17, 5489−5494

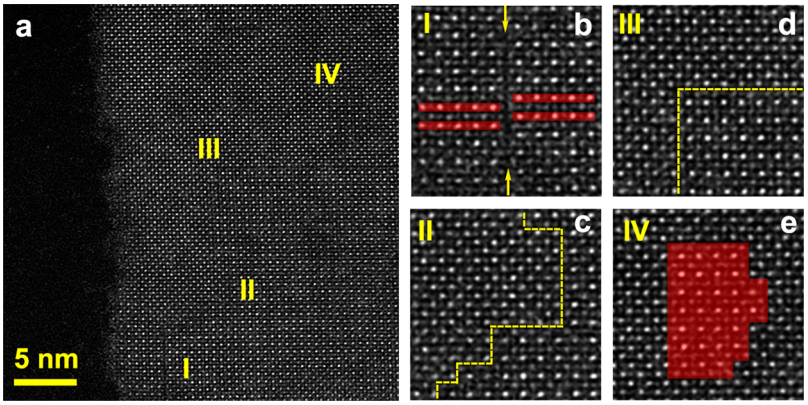

Figure 3. Domain configurations in 2D NSs. (a) AC-STEM image of a typical domain pattern. Four regions are labeled as I–IV. (b) Enlarged image of Region I. Arrows indicate the domain boundary, and the red lines indicate the vertical shift between adjacent lattice planes. (c,d) Enlarged image of Region II and III. Domain boundaries are indicated by yellow dot lines. (e) Enlarged image of Region IV. The perovskite island is highlighted in red.

regions and the enlarged images are shown in Figure 3b–e. In region I, a sharp boundary separates the perovskite phase into two regions, and there is a 1/2 offset of the lattice parameter along the vertical direction between adjacent regions. Therefore, this is a typical antiphase boundary, and it is regarded as a translation boundary defect in the perovskite phase.[16] Regions II and III are the boundary regions between perovskite and RP phase. At first glance from Figure 3a, the domain boundary can be either straight (region III) or zigzag (region II). Looking into details as shown in Figure 3c, one may notice that the zigzag domain boundary is composed of many vertical and horizontal atomic steps. Hence, we can conclude that the sharp domain boundaries between perovskite and RP phase all lay in the ⟨100⟩ direction at the atomic-level. Moreover, we have also observed island-like feature in the NSs. One example is demonstrated in Region IV, where an island of perovskite phase is embedded in the RP phase (highlighted by red).

On the basis of the above observations, we propose the configuration of the 3D domain structure that is shown in Figure 4. For a simple illustration, we have shown the match between one-layer n = 2 RP phase and five-layer perovskite phase, in which case the whole sheet structure has a flat surface. However, it is noteworthy that there is no requirement of flat surface in reality and surface steps could be existed in the NSs. Compared with the cubic structure, the atomic site symmetries are lower in the RP phase. The altered atomic environment

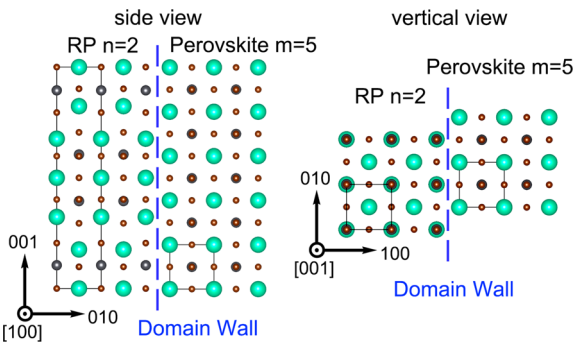

Figure 4. Proposed domain configuration between the conventional perovskite phase and the RP phase. As an example, the match between one-layer RP (n = 2) and cubic perovskite phase (layer thickness m = 5) is demonstrated.

leads to distortions of the atomic distances and of the $PbBr_6$ octahedrons, which is also reflected from our relaxed RP structures obtained by DFT calculations. Such structural alternation is also similar to the case in oxide RP structure.[1] It would be helpful if the side view structure can be directly observed experimentally, as the cases in cross-sectional oxide thin films.[10−12] However, in the 2D NS system, only vertical view can be obtained. Owing to such limitation, further information has to be dug out by quantitative intensity analysis and image simulation.

Figure 5a depicts another typical image where perovskite and plausible RP phase coexist. The domain boundaries have been highlighted, and corresponding regions are labeled. Interestingly, one may notice that the perovskite I region has weak contrast compared with perovskite II region, although they both show the same type of pattern. Meanwhile, although we have demonstrated the atomic-scale imaging of the plausible RP phase, it is still not clear about the exact number of n and the layer thickness. Quantification of the atom column intensities in the AC-STEM image may provide the answers.[17−19] Generally speaking, quantitative elemental and thickness determination can be obtained by either hardware-assisted absolute intensity measurement[17] or model-based postponed data analysis.[18] As to specific materials systems, local thickness measurement in nanostructures could be more challenging than general thickness determination in bulk crystals and thin films. However, without absolute intensity calibration, it is still possible to determine the thickness in certain cases by combining intensity ratio counting and image simulations.[19] To be noted that a full-structure determination including local thickness is really difficult to achieve by intensity counting, and it is still an ongoing topic in the electron microscopy community. Meanwhile, absolute matching between experimental and simulated images are also rather difficult as there are many affecting factors in terms of the experimental contrast as well as the shape of local atom columns. Therefore, we only compared the experimental and simulated images in a semiquantitative way, aiming at digging out more information from our experiments for a better understanding of this system. Here, STEM image simulations were performed using the multislice method.[20,21] The left column of Figure 5b shows the enlarged experimental images from perovskite I, RP, and perovskite II regions, respectively. Correspondingly, the right column of Figure 5b depicts the simulated images showing the

DOI: 10.1021/acs.nanolett.7b02146
Nano Lett. 2017, 17, 5489−5494

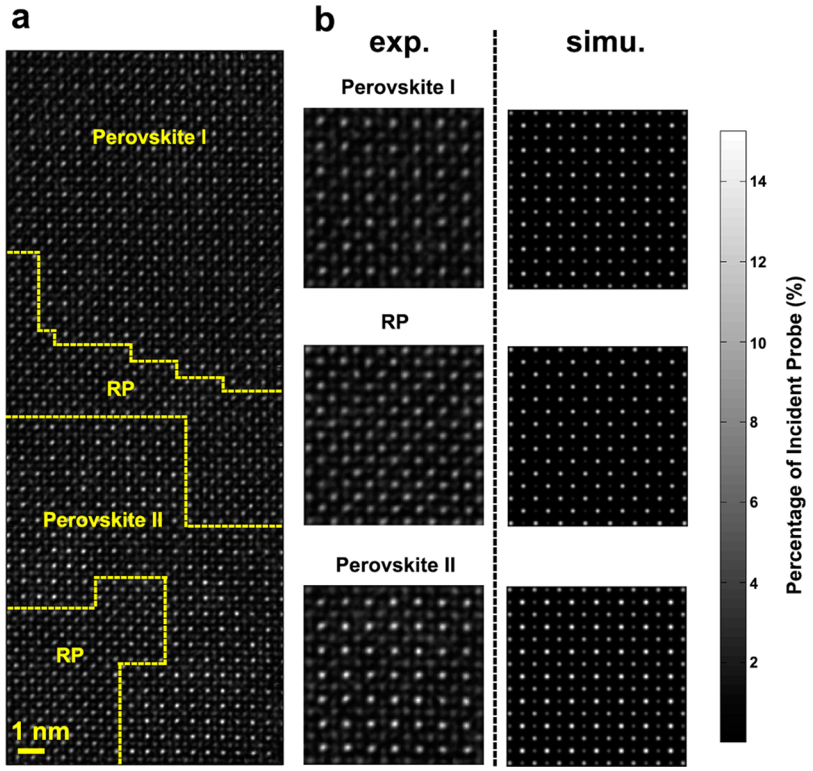

Figure 5. Comparison between experimental and simulated STEM images. (a) Another typical domain region in the NSs. Domain boundaries are indicated by yellow dot lines, and different domains are labeled. (b) Comparison between experimental and simulated images. The left column is the enlarged images from different domains in panel a, and the right column is the corresponding simulated images (six-layer perovskite phase, one-layer n = 2 RP phase, and six-layer perovskite phase with $-PbBr_3$ termination). The simulated intensities have been normalized to the incident probe.

best fit. The simulated intensities have been normalized to the incident probe. Details of the fittings are as follows.

Different thicknesses of perovskite and RP phases have been simulated, and all of the simulated atom column intensities were obtained by 2D Gaussian fitting.[22] The result is shown in Figure 6a. Here we only compare the cation atom column intensities, and the weak Br atom columns are ignored. For the perovskite phase, simulations have been performed from one to ten layers. For RP phases, we only simulate the cases of n = 1 and n = 2 as RP phases with n > 3 may not be thermodynamically stable, according to the lessons we learnt from oxide RP phases.[10] Meanwhile, considering our 2D thin NS system, it is less possible to have RP phases with a higher n number, which would cause a large thickness.

Theoretically, for RP n = 1 phase, from one- to two-layer, intensities of two types of cation atom columns, i.e., I_1 and I_2, are not equal. The difference becomes smaller as the thickness increases from one- to two-layer. Whereas for RP n = 2 phase, I_1 equals to I_2. Besides, both two-layer n = 1 and one-layer n = 2 RP columns show similar but a little weaker intensities compared to the Pb−Br column intensities of four- to six-layer perovskite phase (about 25−35 Å in thickness). Experimentally, within the measurement errors, RP regions show that I_1 equals to I_2, and the experimental intensities of RP atom columns are also a little weaker than the Pb−Br column intensities of perovskite regions. Therefore, it could be possible that the NS in Figure 5a composes of one-layer n = 2 RP phase and 4−6 layers of perovskite phase, so that the thickness of the NS is around 3 nm. To be noted that here we cannot exclusively rule out the possibility of two-layer n = 1 RP phase. However, for a semiquantitative discussion, one-layer n = 2 RP phase is assumed in the following analysis for simplicity.

A further deduction of the thickness can be obtained from the intensity ratio as depicted in Figure 6b. Here, the comparison is made between the perovskite I region and RP region. Three types of intensity ratios have been calculated from one- to ten-layer perovskite phases, while the RP phase is fixed as one-layer n = 2 phase. The experimental values are shown in red, and the error regions, which stand for the standard deviations, are highlighted by orange. As can be seen, the simulations agree well with experiments when the thickness of perovskite phase turns to be five- and six-layer.

For the perovskite II region, it is found that the Pb−Br atom columns show higher intensities compared to perovskite I region while the Cs atom column intensities vary little. Such contrast difference cannot be interpreted by the changes of crystal thickness with integer perovskite layers. Hence, we consider the effect of surface termination.[23] If the perovskite phase does not terminate with integer unit cells, then in the [001] projection, extra Pb and Br atoms will be added into the Pb−Br columns, while the numbers of Cs atoms in Cs columns do not change. In this way, the abnormal intensity features in the perovskite II region can be interpreted. Assuming Perovskite I region is terminated with integer six-layer, we vary the surface terminations of Perovskite II region to best fit the experimental intensity ratio. As depicted in Figure 6c, within the measurement errors, the experimental intensity ratios (red) agree with the simulation of six-layer perovskite phase with either $-PbBr_2$ or $-PbBr_3$ termination. The structures of $-PbBr_2$ or $-PbBr_3$ terminations are demonstrated in the upper region in Figure 6c. Therefore, the perovskite II

DOI: 10.1021/acs.nanolett.7b02146
Nano Lett. 2017, 17, 5489−5494

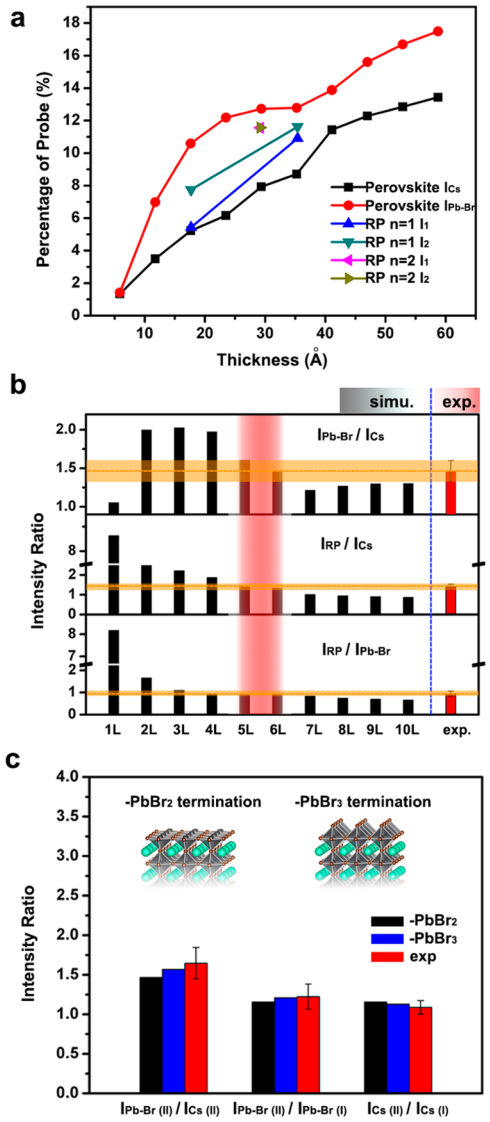

Figure 6. Semiquantitative comparison between experimental and simulated intensity ratios. (a) Simulated cation atom column intensity vs crystal thickness. For perovskite phase, simulations have been performed from one- to ten-layer. For RP phases, one- and two-layer RP (n = 1) and one-layer RP (n = 2) have been simulated. Intensities of two types of cation columns in RP phases are denoted as I_1 and I_2, respectively. (b) Comparison between experimental (red) and simulated (black) intensity ratios (perovskite I and RP regions). In the simulations, the RP phase is fixed as one-layer RP (n = 2), and the perovskite phase thickness ranges from one- to ten-layer. The error bars, representing the standard deviations, are highlighted in orange. The best fit to the perovskite thickness is highlighted in red. (c) Comparison between experimental and simulated intensity ratios (perovskite I and perovskite II regions). Two types of surface terminations, denoted as $-PbBr_2$ and $-PbBr_3$, are considered for Perovskite II region, and their structural models are shown in the inset. The error bars stand for the standard deviations.

region could have six-layer perovskite phase in thickness with Pb and Br-rich surface terminations.

As mentioned, the above comparisons between experiments and simulations are semiquantitative, and the result is not exclusive. On the material side, an assumption has been made that the NSs are not too thick, which is proposed based on the atomic force microscopy measurements[15] and the fact of fast sample damage process under the electron beam. Hence the fittings are restricted in few-layer structures. On the simulation side, residual spherical aberrations and several other trivial effects are not taken into consideration. Even though exclusive composition and thickness determination can not be achieved, the above semiquantitative results may still be helpful, which provide frameworks to help understand the RP structures in this system, at least one possible configuration has been proposed here. Looking ahead, there is pressing need for the synthesis of high yield RP phase inorganic halide perovskites, either in the form of nanostructure or thin film. On one hand, new insights could be gained via microscopic observations from the side view (Figure 4a) in other types of nanostructures. On the other hand, it is expected that, combining low dose techniques to better protect the pristine samples, further structural or spectroscopic information could be obtained for the RP phases. Finally, the successful synthesis and deep structural understanding will make future property measurement and device design possible.

In summary, the plausible existence of RP phases in 2D $CsPbBr_3$ NSs has been supported by atomic-level AC-STEM observations. RP phases and conventional perovskite phases form a domain structure in the 2D NSs system. The features of the domain and domain boundaries have been discussed in detail. RP domains and perovskite domains are well-connected due to their similarity in crystal structures, and all of the domain boundaries lie in the ⟨100⟩ directions at atomic-scale. Combined with simulations, an example of phase and thickness determination within the NSs has been shown, and semiquantitative results could be obtained based on reasonable assumptions. Considering there has been no report of RP phases in inorganic halide perovskites so far, our discovery may open the door for future synthesis of inorganic RP phase halide perovskites and push forward further explorations in this intriguing system.

■ ASSOCIATED CONTENT

Supporting Information

The Supporting Information is available free of charge on the ACS Publications website at DOI: 10.1021/acs.nanolett.7b02146.

Materials synthesis, X-ray diffraction, transmission electron microscopy, image simulation, and first-principles calculation (PDF)

■ AUTHOR INFORMATION

Corresponding Author

*E-mail: p_yang@berkeley.edu.

ORCID

Yi Yu: 0000-0003-4326-5992

Peidong Yang: 0000-0003-4799-1684

Author Contributions

Y.Y. performed TEM experiments, simulations, and data analysis. D.Z. carried out the synthesis of halide perovskite samples. P.Y. supervised the research project. Y.Y. and P.Y. wrote the manuscript. All of the authors discussed the results and commented on the manuscript.

Notes

The authors declare no competing financial interest.

DOI: 10.1021/acs.nanolett.7b02146
Nano Lett. 2017, 17, 5489−5494

■ ACKNOWLEDGMENTS

This work was supported by the U.S. Department of Energy, Office of Science, Office of Basic Energy Sciences, Materials Sciences and Engineering Division, under contract no. DE-AC02-05-CH11231 within the Physical Chemistry of Inorganic Nanostructures Program (KC3103). Work at the NCEM, Molecular Foundry was supported by the Office of Science, Office of Basic Energy Science, of the U.S. Department of Energy under Contract No. DE-AC02-05CH11231. D.Z. would like to acknowledge the fellowship support from Suzhou Industrial Park.

■ REFERENCES

(1) Ruddlesden, S. N.; Popper, P. *Acta Crystallogr.* **1957**, *10*, 538−539.
(2) Dwivedi, A.; Cormack, A. N. *Bull. Mater. Sci.* **1991**, *14*, 575−584.
(3) Battle, P. D.; Blundell, S. J.; Green, M. A.; Hayes, W.; Honold, M.; Klehe, A. K.; Laskey, N. S.; Millburn, J. E.; Murphy, L.; Rosseinsky, M. J.; Samarin, N. A.; Singleton, J.; Sluchanko, N. E.; Sullivan, S. P.; Vente, J. F. *J. Phys.: Condens. Matter* **1996**, *8*, L427−L434.
(4) Birol, T.; Benedek, N. A.; Fennie, C. J. *Phys. Rev. Lett.* **2011**, *107*, 257602.
(5) Oh, Y. S.; Luo, X.; Huang, F. T.; Wang, Y.; Cheong, S. W. *Nat. Mater.* **2015**, *14* (4), 407−413.
(6) Tsai, H.; Nie, W.; Blancon, J. C.; Stoumpos, C. C.; Asadpour, R.; Harutyunyan, B.; Neukirch, A. J.; Verduzco, R.; Crochet, J. J.; Tretiak, S.; Pedesseau, L.; Even, J.; Alam, M. A.; Gupta, G.; Lou, J.; Ajayan, P. M.; Bedzyk, M. J.; Kanatzidis, M. G. *Nature* **2016**, *536*, 312−316.
(7) Stoumpos, C. C.; Cao, D. H.; Clark, D. J.; Young, J.; Rondinelli, J. M.; Jang, J. I.; Hupp, J. T.; Kanatzidis, M. G. *Chem. Mater.* **2016**, *28*, 2852−2867.
(8) Dou, L.; Wong, A. B.; Yu, Y.; Lai, M.; Kornienko, N.; Eaton, S. W.; Fu, A.; Bischak, C. G.; Ma, J.; Ding, T.; Ginsberg, N. S.; Wang, L. W.; Alivisatos, A. P.; Yang, P. *Science* **2015**, *349*, 1518−1521.
(9) Takeoka, Y.; Asai, K.; Rikukawa, M.; Sanui, K. *Bull. Chem. Soc. Jpn.* **2006**, *79*, 1607−1613.
(10) Wang, P.; Bleloch, A. L.; Yan, L.; Niu, H. J.; Chalker, P. R.; Rosseinsky, M. J.; Goodhew, P. J. *J. Phys. Conf. Ser.* **2008**, *126*, 012050.
(11) Zhu, Y.; Lee, C. H.; Schlom, D. G.; Muller, D. A. *Microsc. Microanal.* **2011**, *17*, 1396−1397.
(12) Riedl, T.; Gemming, T.; Weissbach, T.; Seifert, G.; Gutmann, E.; Zschornak, M.; Meyer, D. C.; Gemming, S. *Ultramicroscopy* **2009**, *110*, 26−32.
(13) Gonze, X.; Amadon, B.; Anglade, P. M.; Beuken, J. M.; Bottin, F.; Boulanger, P.; Bruneval, F.; Caliste, D.; Caracas, R.; Côté, M.; Deutsch, T.; Genovese, L.; Ghosez, P.; Giantomassi, M.; Goedecker, S.; Hamann, D. R.; Hermet, P.; Jollet, F.; Jomard, G.; Leroux, S.; Mancini, M.; Mazevet, S.; Oliveira, M. J. T.; Onida, G.; Pouillon, Y.; Rangel, T.; Rignanese, G. M.; Sangalli, D.; Shaltaf, R.; Torrent, M.; Verstraete, M. J.; Zerah, G.; Zwanziger, J. W. *Comput. Phys. Commun.* **2009**, *180*, 2582−2615.
(14) Zhang, D.; Eaton, S. W.; Yu, Y.; Dou, L.; Yang, P. *J. Am. Chem. Soc.* **2015**, *137*, 9230−9233.
(15) Yu, Y.; Zhang, D.; Kisielowski, C.; Dou, L.; Kornienko, N.; Bekenstein, Y.; Wong, A. B.; Alivisatos, A. P.; Yang, P. *Nano Lett.* **2016**, *16*, 7530−7535.
(16) Zurbuchen, M. A.; Tian, W.; Pan, X. Q.; Fong, D.; Streiffer, S. K.; Hawley, M. E.; Lettieri, J.; Jia, Y.; Asayama, G.; Fulk, S. J.; Comstock, D. J.; Knapp, S.; Carim, A. H.; Schlom, D. G. *J. Mater. Res.* **2007**, *22*, 1439−1471.
(17) LeBeau, J. M.; Findlay, S. D.; Allen, L. J.; Stemmer, S. *Phys. Rev. Lett.* **2008**, *100*, 206101.
(18) Van Aert, S.; Verbeeck, J.; Erni, R.; Bals, S.; Luysberg, M.; Van Dyck, D.; Van Tendeloo, G. *Ultramicroscopy* **2009**, *109*, 1236−1244.
(19) Ortalan, V.; Uzun, A.; Gates, B. C.; Browning, N. D. *Nat. Nanotechnol.* **2010**, *5*, 843−847.
(20) Kirkland, E. J. *Advanced Computing in Electron Microscopy*; Springer: New York, 2010.
(21) Koch, C. *Determination of core structure periodicity and point defect density along dislocations*. Ph.D. Thesis, Arizona State University, 2002.
(22) Sang, X.; Oni, A. A.; LeBeau, J. M. *Microsc. Microanal.* **2014**, *20*, 1764−1771.
(23) Haruyama, J.; Sodeyama, K.; Han, L.; Tateyama, Y. *J. Phys. Chem. Lett.* **2014**, *5*, 2903−2909.

DOI: 10.1021/acs.nanolett.7b02146
Nano Lett. 2017, 17, 5489−5494